PERGAMON

International Journal of Solids and Structures 40 (2003) 73–88

INTERNATIONAL JOURNAL OF SOLIDS and STRUCTURES

www.elsevier.com/locate/ijsolstr

Force recovered from three recorded strains

E. Jacquelin *, P. Hamelin

Laboratoire Mécanique Matériaux Université Claude Bernard Lyon I Domaine universitaire de la Doua—IUT A Génie civil F-69622, Villeurbanne Cedex, France

Received 6 February 2002; received in revised form 29 August 2002

Abstract

To improve the dynamic behaviour of some structural elements, a well-adapted setup must be developed. The split Hopkinson pressure bar device is well-known for its application in dynamic tests on materials. To test structural elements, the energy of impact must be increased and direct impact may be used. That is the principle of the 'block-bar' device, which allows reconstruction of the crushing force on a sample. Nevertheless, the duration of the experimental impact is so long that it is not an obvious task to recover the force well. Lundberg has proposed equations for the reconstruction. Unfortunately, Lundberg's method has some limitations. In this paper, the limitations are highlighted and new methods are proposed to overcome the problems. More precisely, new equations are proposed to recover the force directly from strain measurements at three given sections of the measuring bar. This method avoids numerical problems. Moreover, the problems and the methods are always viewed from the frequency and the time perspectives. The duality between time and frequency is present throughout this article. In this approach, a problem (or a method) in time domain has an equivalent in frequency domain and vice versa.

Keywords: Split Hopkinson pressure bar; Force reconstruction; Wave propagation

1. Introduction

To perform tests under static loading, some simple apparatuses and techniques can be used. In these tests, force, displacement and strain are directly recorded by force or displacement sensors or by gauges. Dynamic tests of materials or structures are more difficult to conduct because the signals are often recovered by indirect measurements. That is the case with the split Hopkinson pressure bar (SHPB) which is a standard experimental setup for testing materials under dynamic loading. This technique is due to Hopkinson (1914) and has been studied and developed by Davies (1948) and by Kolsky (1963).

The measuring technique for a SHPB involves the recording of the histories of strains in different sections for reconstructing the histories of the stresses and strains in the specimen tested. To state briefly, the knowledge of the strains in some sections gives the strains due to the waves propagating in opposite

* Corresponding author. Tel.: +33-4-72-69-21-30; fax: +33-4-78-94-69-06.
E-mail address: jac@iutal2m.univ-lyon1.fr (E. Jacquelin).

0020-7683/02/$ - see front matter © 2002 Elsevier Science Ltd. All rights reserved.
PII: S0020-7683(02)00544-9

directions. These strain profiles can be used to evaluate the force and the velocity at any section. Theoretically, the force could be obtained with one strain-gauge glued near the end of the bar in contact with the specimen. In practice, this method is not accurate (Saint–Venant principle). The principle of the Hopkinson's bars is based on the wave propagation in a one-dimensional medium. The simplicity of the method has certainly contributed to its success. Moreover, it allows not only compression tests, but also tensile and torsional loadings. The first corrections deal with the dispersion Follansbee and Frantz (1983), Gorham et al. (1992), etc.) associated with the three-dimensional effects (Dharan and Hauser (1970)) to improve the accuracy.

Nevertheless, the SHPB is limited with regard to the energy of impact and the length of the sample. Indeed, if the energy of impact is too high, the elastic yield may be exceeded: a plastic wave could propagate. Moreover, to recover the strains in any section, the two elementary waves propagating in opposite directions must be known: then, the duration of the measurements and the length of the pulse are limited. This is a great limitation: some structures (as absorbers of energy, currently used in the automotive industry) cannot be tested. To overcome these difficulties, we use another setup called 'block-bar' (Jacquelin and Hamelin (2001)) in conjunction with the 'Lundberg equations' given by Lundberg and Henchoz (1977). Then, the energy and the duration of impact are not limited. Unfortunately, the latter equations don't take into account the dispersion (that limits the accuracy for a long duration of measurement) and make impossible to recover some frequency components of the signal of interest. These problems have been pointed out by several authors (Zhao and Gary (1997), Bacon (1999), Jacquelin and Hamelin (2001), etc.). Firstly, Zhao and Gary (1997) have proposed a method to take into account the dispersion; Bacon (1999) has given another approach to recover the whole spectrum of the signal. Finally, the BCGO-method has been developed by Othman et al. (2001), Bussac et al. (2002) to overcome all the difficulties and to optimize the solution with regard to the measurement noise.

This article deals with an alternative method to the BCGO-method: the proposed methods are extremely simple and easy to program. As those methods will be compared, BCGO-method will also be presented. Indeed, the method allows to recover all the frequency components of the force or, if we prefer to work in time domain, it does not increase any measurement noise.

Note that this article is not focused on the number of measurement points used: the objective is to obtain a method free from the limitations associated with the Lundberg equations but based on the same assumptions.

Firstly, the block-bar device, the Lundberg equations and the difficulties inherent to them are recalled.

2. Block-bar device: setup, theory and limitations

2.1. Experimental setup

The principle of this experimental setup is rather simple. A projectile is hurled with the help of a compressed air gun and impacts the sample to test. This one is stuck to an end of a bar. Thus, as shown in Fig. 1, the block-bar is composed of three parts:

- a compressed air gun and a projectile,
- a measuring bar and instrumentation,
- a hydraulic shock absorber.

The 5 m long gun is fed with compressed air from the laboratory system ($P_{max} = 7$ bars) and allows the use of projectiles which vary up to 300 kg in weight. The incident speed of the projectile can reach 20 m/s. A high-velocity hydraulic jack triggers the shot of air contained in the tank; by adjusting the pressure, this

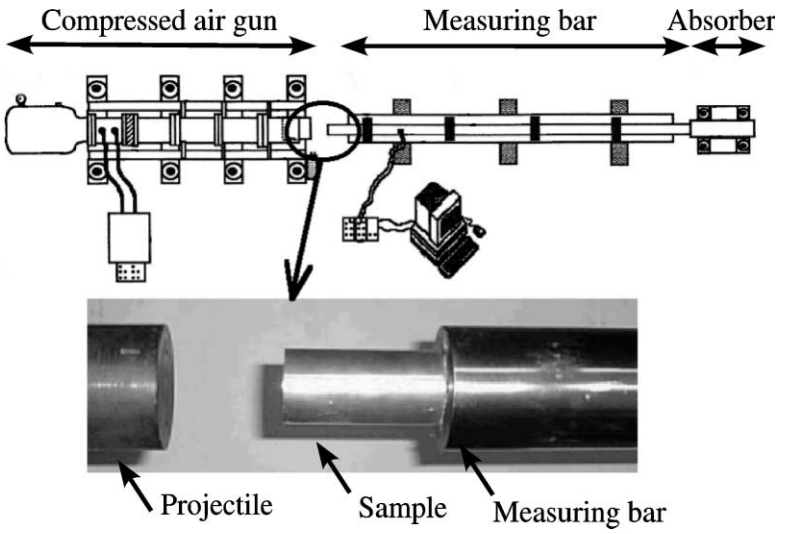

Fig. 1. Block-bar setup.

allows a good reproducibility of the impact. A system of optical measurement allows us to know the projectile speed at the time of impact on the sample. The measuring bar is 80 mm in diameter and 4 m long. All the measurements are carried out by two strain-gauges bridges glued onto the bar. The signals are collected by differential amplifiers and an oscilloscope board allows us to record 500000 data at a sampling rate which can be of 200 kHz to 2 MHz.

The hydraulic shock absorber stops the measuring bar after the test; during the test, the bar is free.

The objective of this setup is to determine the crushing force of the sample. Consequently, the strain (then the force) at the impacted end, must be recovered.

2.2. Theory

This experimental setup allows the determination of the strain and the velocity in each section of the measuring bar. In fact, the strains $\epsilon_A(t)$ and $\epsilon_B(t)$ are recorded at two different sections of the bar and Lundberg and Henchoz (1977) has proposed some simple equations to recover the strain and the velocity at any section of the bar. They are based on the longitudinal elastic wave propagation in rods. Thus, for the strain and the velocity at the impacted end 0 these ones are such as:

- Strain

$$\epsilon_0(t+2T) = \epsilon_0(t) + \epsilon_A(t+T_A+2T) - \epsilon_A(t-T_A) + \epsilon_B(t-T_A+T) - \epsilon_B(t+T_A+T) \quad \text{for } t \geqslant 0 \qquad (1)$$

$$\epsilon_0(t) = \epsilon_A(t+T_A) \text{ for } t \in [0, 2T]$$

Then, we can also determine the force $F_0(t) = ES\epsilon_0(t)$ at the impacted end of the bar.

- Velocity

$$v_0(t+2T) = v_0(t) + c_0(-\epsilon_A(t+T_A+2T) - \epsilon_A(t-T_A) + \epsilon_B(t-T_A+T) + \epsilon_B(t+T_A+T_B) \quad \text{for } t \geqslant 0 \qquad (2)$$

$$v_0(t) = -c_0\epsilon_A(t + T_A) \quad \text{for } t \in [0, 2T]$$

where

- c_0: speed of elastic longitudinal wave,
- $T_A = x_A/c_0$; $x_A = 1.1$ m is the position of the section A,
- $T = (x_B - x_A)/c_0$; $x_B = 2$ m is the position of the section B,
- $T_B = T_A + T$
- E, S: Young's modulus and cross-sectional area of the measuring bar.

Note that 0 is the origin of the system of reference ($x_0 = 0$).

A "one-point" measurement method has even been proposed if a free end is used as the second measurement point by Park and Zhou (1999).

Those equations are based on an elastic one-dimensional medium, but in practice, the medium is not one-dimensional and then the medium is a dispersive one: the speed of the elastic longitudinal waves is a function of the frequency.

2.3. Limitations: frequency point of view

To solve a recursive equation like the Lundberg's ones, it is useful to work in frequency domain. That is why it is interesting to apply the Fourier transform to Eqs. (1) and (2). Then, after some calculations, the associated frequency equation is obtained. Thus relation (1) becomes:

$$E_0(\omega) = \frac{E_A(\omega)\sin(\omega T_B) - E_B(\omega)\sin(\omega T_A)}{\sin(\omega T)} \tag{3}$$

where $E_i(\omega)$ is the Fourier transform of $\epsilon_i(t)$.

As remarked by some authors Bacon (1999), Jacquelin and Hamelin (2001), Zhao and Gary (1997), the denominator becomes null for the following frequencies:

$$f_k = \frac{k}{2T} \tag{4}$$

Remark 1. A fine analysis of Eq. (3) allows to conclude that, if there is no noise, expression (3) is defined whatever the frequency. Indeed, only if there is no noise, the denominator and the numerator are cancelled at the frequencies f_k: a Taylor expansion of $E_0(\omega)$ proves that $E_0(2\pi f_k)$ can be defined by continuity. Unfortunately, in practice, the signals are spoiled by the measurement noise: consequently, the f_k are effectively some poles of E_0. Then, we face a frequency limitation: the technique cannot recover some frequency components of ϵ_0. Note that this limitation is a function of the relative position of the gauges.

2.4. Limitations: time point of view

The latter limitation cannot be overcome by solving the Lundberg equation in time domain. It is obvious that the frequency limitation has an equivalent limitation in time domain. In fact, in time domain, the problem is due to the recursiveness of the Lundberg equations, as shown by the following calculations:

$$\begin{aligned}\epsilon_0(k\Delta t) &= \epsilon_0(k\Delta t - 2T) + \epsilon_A(k\Delta t + T_A) + \Delta\epsilon_A(k\Delta t + T_A) - \epsilon_A(k\Delta t - T_B - T) - \Delta\epsilon_A(k\Delta t - T_B - T)\\ &\quad + \epsilon_B(k\Delta t - T_B) + \Delta\epsilon_B(k\Delta t - T_B) - \epsilon_B(k\Delta t + T_A - T) - \Delta\epsilon_B(k\Delta t + T_A - T)\\ &= \epsilon_0(k\Delta t - m \times 2T) + \sum_{l=0}^{m-1} \epsilon_A(k\Delta t - l \times 2T + T_A) - \epsilon_A(k\Delta t - l \times 2T - T_B - T)\\ &\quad + \epsilon_B(k\Delta t - l \times 2T - T_B) - \epsilon_B(k\Delta t - l \times 2T + T_A - T) + \sum_{l=0}^{m-1} \Delta\epsilon_A(k\Delta t - l \times 2T + T_A)\\ &\quad - \Delta\epsilon_A(k\Delta t - l \times 2T - T_B - T) + \Delta\epsilon_B(k\Delta t - l \times 2T - T_B) - \Delta\epsilon_B(k\Delta t - l \times 2T + T_A - T)\end{aligned} \tag{5}$$

where

- m is an integer such as $m \leqslant k\Delta t/2T < m + 1$,
- $\Delta\epsilon_X$ ($X = A$ or B) is the inherent noise associated with the measurement $\tilde{\epsilon}_X(t)$ of the function $\epsilon_X(t)$:

$$\tilde{\epsilon}_X(t) = \epsilon_X(t) + \Delta\epsilon_X(t)$$

Eq. (5) shows that:

(1) the perturbation due to the noise increases with the index k; the period of this amplification is $2 \times T$: this corresponds to the frequency limitation viewed previously,
(2) for perfect data (i.e without noise), the reconstruction is perfect.

Then the same features are found whatever the domain (time or frequency domain) used: that is clear for the conclusion 1. Moreover, the Remark 1 above allows to conclude that, theoretically, in frequency domain, for perfect data (i.e without noise), the reconstruction is perfect.

3. The BCGO-method

This method is based on calculations in frequency domain (to take into account the dispersion) and requires N strain and P velocity measurements Othman et al. (2001), Bussac et al. (2002). The objective is to determine the waves propagating ($A(\omega)$ and $B(\omega)$) in the opposite directions. Then the strain and the velocity in any section x can be calculated in frequency domain:

$$E(x,\omega) = A(\omega)\mathrm{e}^{-\xi(\omega)x} + B(\omega)\mathrm{e}^{\xi(\omega)x}$$

$$\widetilde{V}(x,\omega) = \frac{-\omega}{\xi(\omega)}A(\omega)\mathrm{e}^{-\xi(\omega)x} + \frac{\omega}{\xi(\omega)}B(\omega)\mathrm{e}^{\xi(\omega)x}$$

where ξ is the wave number.

The measured strains $\tilde{\epsilon}_i(t)$ and velocities $\tilde{v}_i(t)$ at the sections x_i are assumed such as:

$$\tilde{\epsilon}(x_i,t) = \epsilon(x_i,t) + \Delta\epsilon_i(t)$$

$$\tilde{v}(x_i,t) = v(x_i,t) + \Delta v_i(t)$$

where the noises $\Delta\epsilon_i(t)$ and $\Delta v_i(t)$ are statistically independent white noises.

The functions $A(\omega)$ and $B(\omega)$ are those which minimise the Maximum Likelihood functional $\mathscr{F}$:

$$\mathscr{F} = \frac{1}{2\pi}\int\left(\sum_{i=1}^{N}\left|\widetilde{E}(x_i,\omega) - A(\omega)\mathrm{e}^{-\xi(\omega)x_i} - B(\omega)\mathrm{e}^{\xi(\omega)x_i}\right|^2 + \sum_{i=1}^{P}\left|\widetilde{V}(x_i,\omega) - \frac{-\omega}{\xi(\omega)}A(\omega)\mathrm{e}^{-\xi(\omega)x_i} - \frac{\omega}{\xi(\omega)}B(\omega)\mathrm{e}^{\xi(\omega)x_i}\right|^2\right)\mathrm{d}\omega$$

After some calculations, the solutions are expressed as a rational fraction Bussac et al. (2002):

$$A(\omega) = \frac{\mathscr{N}_A(\widetilde{E}(x_i,\omega),\widetilde{V}(x_i,\omega),\xi,x_i,\omega)}{\mathscr{D}_A(\xi,x_i,\omega)}$$

$$B(\omega) = \frac{\mathscr{N}_B(\widetilde{E}(x_i,\omega),\widetilde{V}(x_i,\omega),\xi,x_i,\omega)}{\mathscr{D}_B(\xi,x_i,\omega)}$$

As the denominators $\mathscr{D}_A$ and $\mathscr{D}_B$ may cancel each other out, a small damping is introduced (the wave number becomes a complex number). If $N \geqslant 3$, the results are independent of this value; the two gauges solution is not better than the Lundberg solution.

The solution obtained is an optimal one as regards the noise. This is why the BCGO is so interesting. Nevertheless, the mathematical developments make it long to implement. This is why an other solution is proposed.

4. The 3-gauges method

4.1. The frequency point of view

The frequency limitation is linked to the position of the measurement points A and B:

$$f_k^{(A,B)} = \frac{c(f_k)}{2(x_B - x_A)}$$

Consequently, it is natural to use a third 'well-positioned' C point, i.e. such as $f_k^{(A,B)}$, $f_k^{(A,C)}$ and $f_k^{(B,C)}$ are incommensurable two by two. Then, for each frequency, it always exists a pair of points which allows to determine the frequency component of the signal.

In practice, three pairs of measurements are available in time domain: $(\epsilon_A(t), \epsilon_B(t))$, $(\epsilon_B(t), \epsilon_C(t))$ and $(\epsilon_C(t), \epsilon_A(t))$. Then, by discrete Fourier transform, three pairs of spectra can be used $((E_A(\omega), E_B(\omega))$, $(E_B(\omega), E_C(\omega))$ and $(E_C(\omega), E_A(\omega)))$ to recover the spectrum $E_0(\omega)$ with the help of the Eq. (3). Then, for each frequency f_i, three values of $E_0(2\pi f_i)$ are obtained: $E_0^{(A,B)}(2\pi f_i)$, $E_0^{(B,C)}(2\pi f_i)$ and $E_0^{(C,A)}(2\pi f_i)$. If f_i is not a critical frequency, the three values are, theoretically, almost similar: the average of these values is the final value. If f_i is a critical frequency for one pair, the value associated with this pair is not used to determine the final value: if the point C is well chosen, we know that f_i is not critical for one pair at least.

Note that in theory, except for the critical frequencies, the spectra must be equal whatever the pair of points used. Indeed, as shown in Fig. 2, except for a discrete set of frequencies (the critical frequencies associated to the three pairs of gauges), the spectra are almost the same.

4.2. The time point of view

The previous subsection indicates that, in theory, it is possible with 3-gauges to eliminate the limitations of the Lundberg equations when frequency considerations are used. Consequently, it must exist an

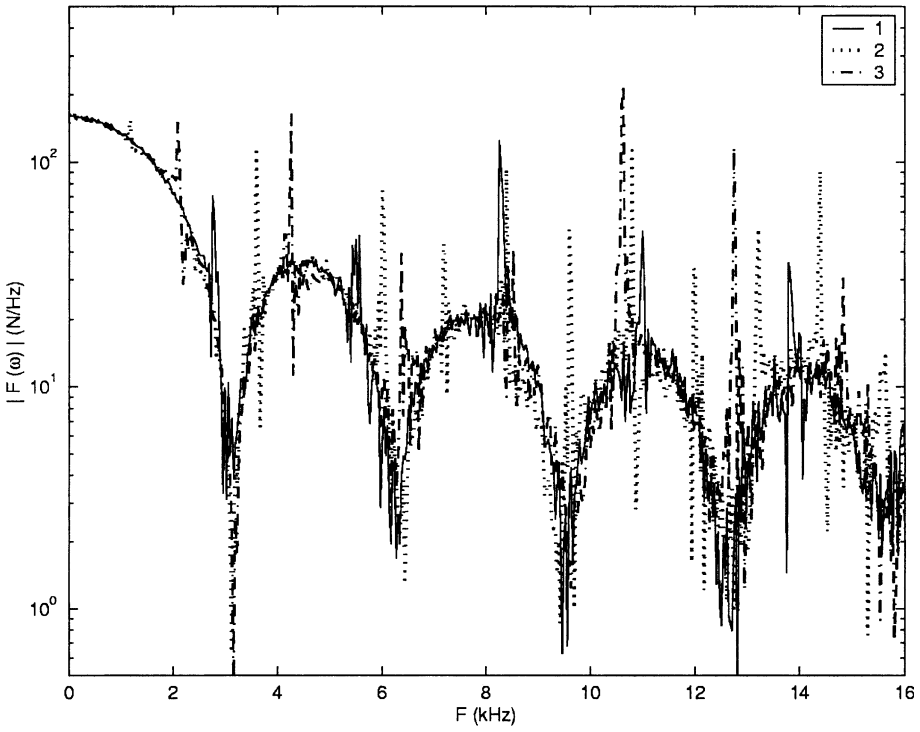

Fig. 2. Spectra of the calculated force for three pairs of gauges.

equivalent method in time domain such as, with three well-positioned gauges, it is possible to overcome the limitations. Then, it must exist some equations similar to Lundberg's ones, that can allow to recover directly the strain in one section with the measurements at three other sections.

Indeed those relations exist: it can be proved (see in Appendix A) that:

$$\epsilon_0(t) = \frac{1}{2}\{\epsilon_A(t - T_A) + \epsilon_A(t + T_A) + \epsilon_B(t - T_B) + \epsilon_B(t + T_B) - \epsilon_C(t + T_B - T_A) - \epsilon_C(t - T_B + T_A)\} \tag{6}$$

$$\frac{v_0(t)}{c_0} = \frac{1}{2}\left\{\epsilon_A(t - T_A) - \epsilon_A(t + T_A) + \epsilon_B(t - T_B) - \epsilon_B(t + T_B) + \frac{v_C(t + T_B - T_A)}{c_0} + \frac{v_C(t - T_B + T_A)}{c_0}\right\} \tag{7}$$

with the point C such as

$$x_C - x_B = x_A - x_0$$

Then, if the C point has the previously determined position, it is possible to recover the signals in a given point 0 without any limitations: the latter equations are not recursive ones, and then, the errors cannot be propagated. That is the great advantage of those equations over the other methods.

Eq. (7) shows that to determine the velocity at a point 0, a velocity must be measured at the point C: in practice, a such measurement is not easy.

In our real setup, the C point is the free end of the bar: $\epsilon_C \equiv 0$. Then, the points A and B are the same and are located at the mid-length of the bar. Eq. (6) becomes:

$$\epsilon_0(t) = \epsilon_B(t + T_B) + \epsilon_B(t - T_B) \tag{8}$$

If the medium is supposed to be dispersive, expression (8) must be written in frequency domain by Fourier transform:

$$E_0(\omega) = E_B(\omega)\mathrm{e}^{\mathrm{i}\omega T_B} + E_B(\omega)\mathrm{e}^{-\mathrm{i}\omega T_B} \tag{9}$$

The latter equation is clearly available for each frequency: the latter expression also proves that there is effectively no limitation.

It is worth to note the difference between Eqs. (6) and (7) and the Lundberg equations: the whole equations are exact, but the Lundberg equations are recursive. Then, solving these equations is an inverse problem which can be written as a deconvolution problem, i.e. as an ill-posed problem. The new Eqs. (6) and (7) are not recursive: the strain at '0' is directly obtained without any linear system solving. Then, the solution is not spoiled by a 'numerical noise'.

5. Results

To validate and compare the methods, some purely numerical simulations are used to control the experimental noise. Then, a real experiment is performed and the results are compared again.

Table 1
Location of the measurement points

Point	0	*A*	*B*	*C*	*F*
Position (m)	0	1.1	2	3.1	4

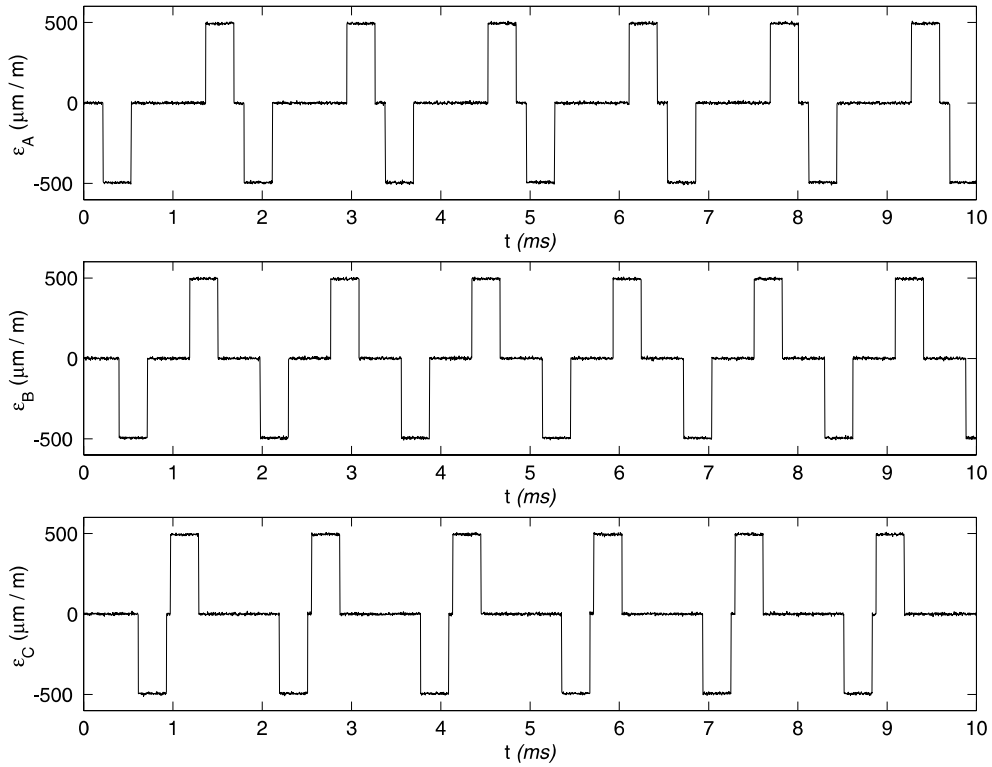

Fig. 3. Noisy strains (points *A*, *B* and *C*).

5.1. Numerical simulations

In order to prevent the interference of multiple problems, the dispersive feature of the medium is not taken into account. Then the waves produced by a given known loading strain (a rectangular pulse) at one end of the bar, are built at three given measurement points A, B and C: this simulates the three recorded strains. The other end of the bar is stress-free: the strains are equal to zero. The location of the different points are given in Table 1. The points 0 and F are the loaded and free (respectively) ends of the bar; A and B correspond at the measurement points of the real setup. To see an influence of the noise, the strains are then spoiled by a gaussian noise (average null-standard deviation: 1% of the maximum of the strains). The noisy strains at A, B and C are shown in Fig. 3. To test the quality of a procedure, we try to recover the rectangular pulse of force F_0 and the zero-force F_F respectively at the loaded and the stress-free ends of the bar. The quality is given by the two following error measurements:

$$\text{Excited end: } \mathscr{E}_0 = \frac{\|F_{\text{recovered}} - F_{\text{initial}}\|_2}{\|F_{\text{initial}}\|_2}$$

$$\text{Stress-free end: } \mathscr{E}_F = \frac{\|F_{\text{recovered}}\|_2}{N}$$

where N is the number of time steps.

In Fig. 4, it is interesting to see the amplification of the noise with the Lundberg's equation: as the time increases, the maximum of the strains increases too. Moreover, this figure also shows how difficult it is to recover a null force at the stress-free end. The BCGO method proves its efficiency with Fig. 5: the

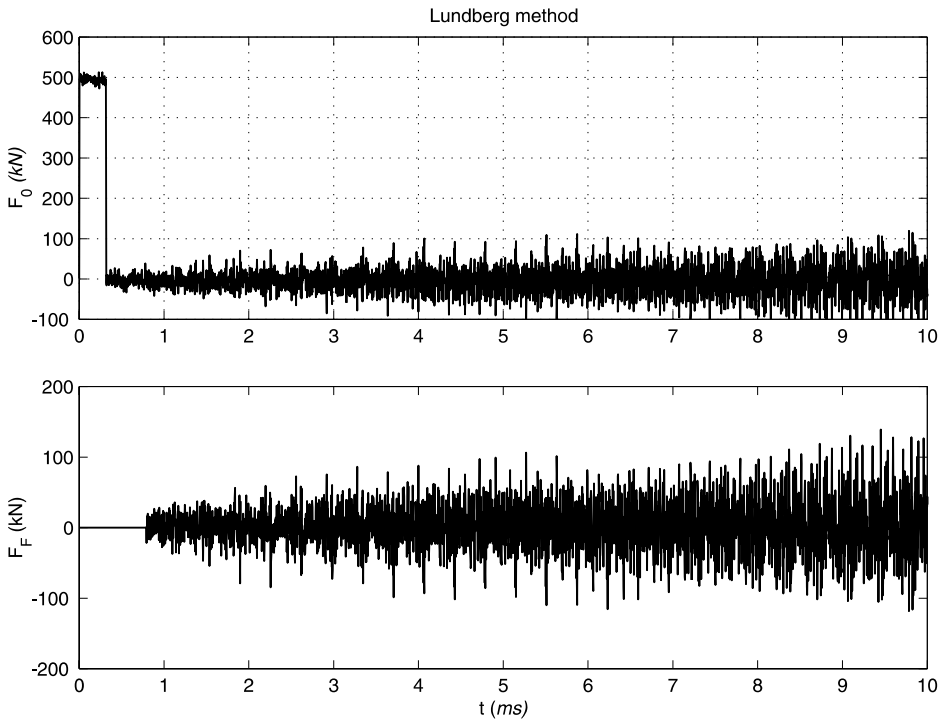

Fig. 4. Forces recovered at the ends of the bar from the Lundberg method.

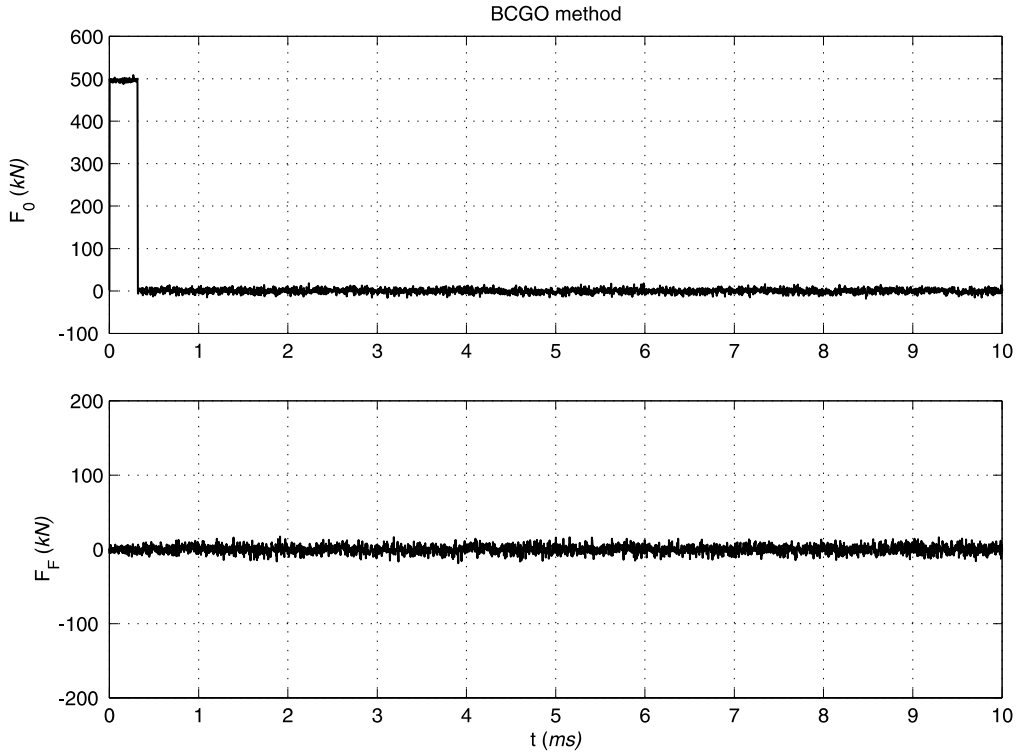

Fig. 5. Forces recovered at the ends of the bar from the BCGO method.

rectangular pulse is described well and the force is almost null after the pulse of force. The 'frequency 3-gauges' method is clearly better than the Lundberg equations, as it is shown in Fig. 6. Particularly, note that the force at the stress-free end is not so high. Nevertheless, the rectangular pulse is not as well recovered as in the BCGO method. Fig. 7 shows that the 'time 3-gauges' method seems to be as good as the BCGO method. Indeed, Table 2 indicates that $\mathscr{E}_0$ are rather similar in the BCGO and 'time 3-gauges' methods; the $\mathscr{E}_F$ criterium shows a better quality for the BCGO method.

In conclusion, this numerical test proves that, even if the BCGO method is the better method, the 'time 3-gauges' and the 'frequency 3-gauges' are good ones. With that three methods, the Lundberg limitations are effectively overcome.

5.2. Experimental data

A block-bar device is specially well-adapted to test absorbers of energy such as the ones used by the automotive industry. So the different methods are used to recover the crushing force of a multimaterial absorber: this one is an aluminium circular tube externally reinforced by carbon-epoxy composite material (see the characteristics in Tables 3 and 4).

Fig. 8 shows the good quality of the force recovered by the BCGO, time 3-gauges and frequency 3-gauges method. These methods allow to calculate the mean crushing force which represents the specific energy absorption and then to compare different absorbers. That is not so easy with the Lundberg method: the results are spoiled by the noise due to the limitation of the method.

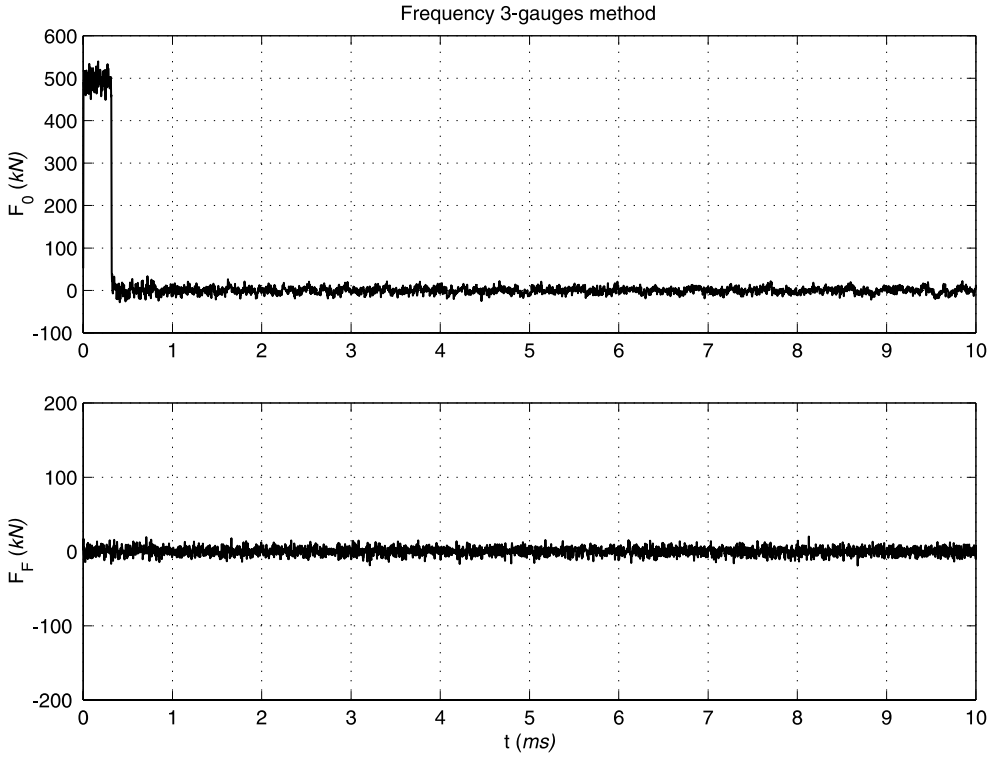

Fig. 6. Forces recovered at the ends of the bar from the "frequency 3-gauges" method.

If we try to superpose on the different curves of Fig. 8, the following features may be noted:

- no real difference can be viewed between the BCGO and the time 3-gauges methods,
- the frequency 3-gauges underestimate slightly the force as regards the BCGO method.

6. Discussion

6.1. Dispersion

The latter simulations and calculations do not take into account the three-dimensional aspect of the bar: it is why the medium does not appear dispersive. Thus, the speed of waves does not depend on frequency: it is equal to c_0. It is not the case in fact. Nevertheless, the whole methods can take into account this feature. The frequency methods (BCGO and frequency 3-gauges) are well-adapted for the dispersive media: c_0 must be changed by $c(f)$. For the other methods, we must take the Fourier transform of the equations (see expression (9)), and then work in frequency domain: in practice, it is not a problem to take into account the dispersive effects.

6.2. Comparison between BCGO and the 3-gauges methods

The quality of the results obtained by the BCGO and time 3-gauges methods is similar. This is interesting because their objective is different:

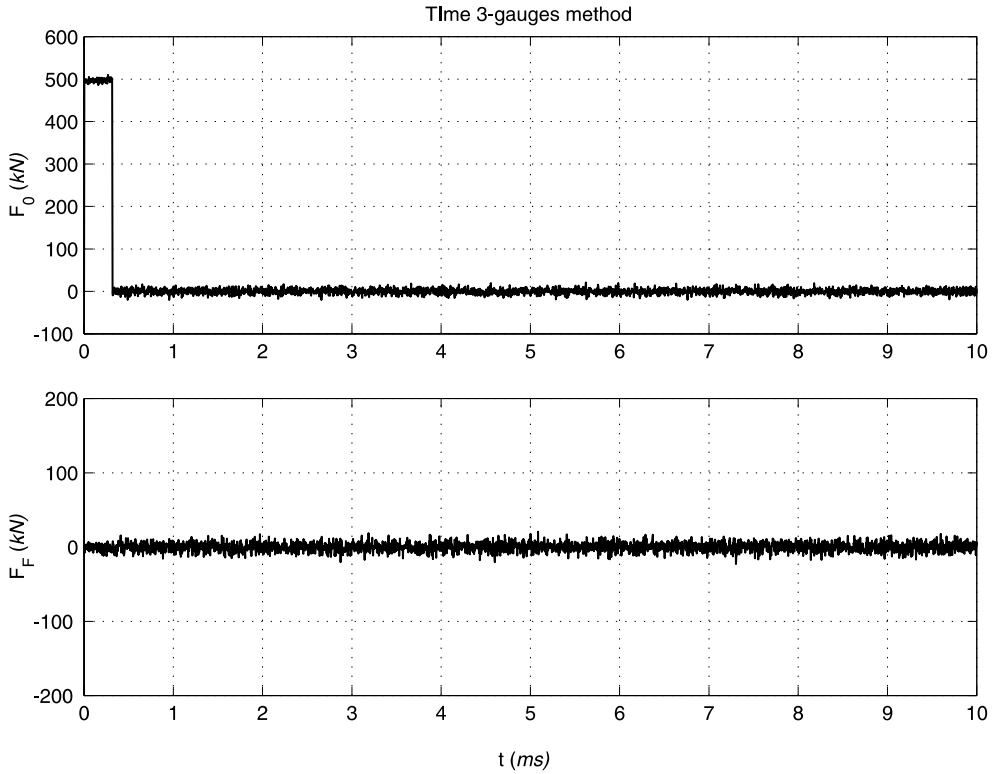

Fig. 7. Forces recovered at the ends of the bar from the "time 3-gauges" method.

Table 2
Differences between recovered and initial forces

	Lundberg	BCGO	Frequency 3-gauges	Time 3-gauges
Excited end (%)	39.9	6.0	9.5	6.9
Stress-free end (N)	622.4	93.9	115.0	106.9

Table 3
Characteristics of the aluminium absorber

Young's modulus (GPa)	Density (kg/m^3)	Height (mm)	Ext. diameter (mm)	Thickness (mm)
70	2670	100	50	2

Table 4
Characteristics of the composite material

	Young's modulus	Ultimate stress	Mass by surface unit of fibres
Carbon HR	90 GPa	1300 MPa	300 ± 3 g/m^2
Epoxy	3.2 MPa	85 MPa	

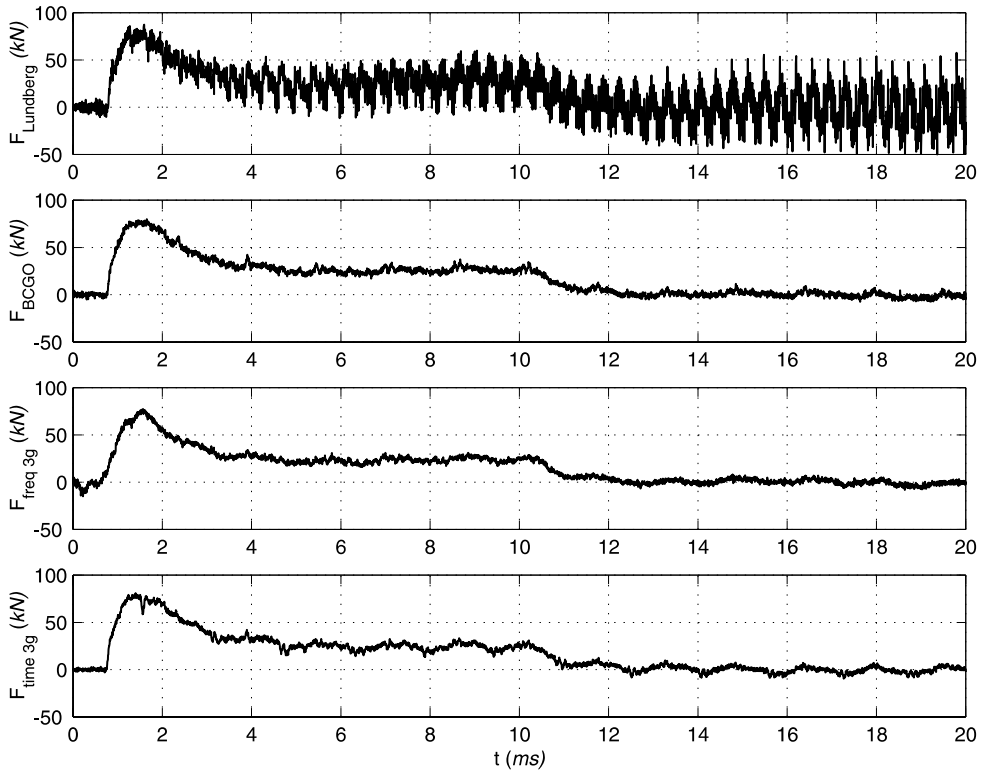

Fig. 8. Crushing force of a tubular multimaterial absorber of energy.

- the BCGO method searches an optimal solution regarding the measurement noise,
- the time 3-gauges method provides an exact non-recursive relation between 3 recorded strains and the required strain: the solution is exact when there is no measurement noise.

The first method gives more informations because, the incident $A(\omega)$ and reflected $B(\omega)$ are determined. Then, the strain and the velocity at any section of the bar may be evaluated. With the time 3-gauges method, the velocity at the measurement point C is required: that is not easy, because the velocity measurement is not as accurate and easy as for the strain measurement. A simple manner to determine the velocity accurately consists in clamping one end of the measurement bar. The velocity at this point is then known: this end must be the point C. Nevertheless, the time 3-gauges method is sufficient because the strains at the impacted end must be solely determined to recover the crushing force of the tested sample. Moreover, this method is far too simpler to implement than the BCGO method.

The frequency 3-gauges method is not as accurate as the two previous methods. This is due to the difficulty in detecting the division by zero, i.e. a peak. In fact, this peak is not located at one frequency: some frequencies around a central frequency must be often eliminated too. The problem is to determine the number of frequency components that must be "forgotten" to recover the spectrum of the signal. Nevertheless, this method can be very interesting if the velocity is required: if the 'time 3-gauges' method is interesting with a free-clamped measuring bar, for the other boundary conditions, the frequency 3-gauges must be used to determine the velocity.

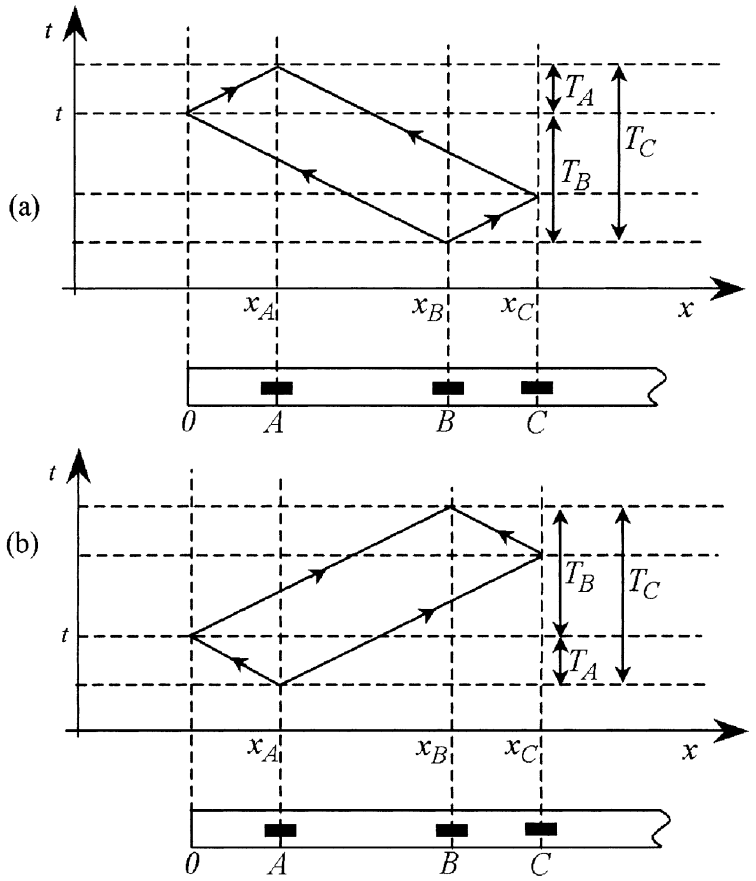

Fig. 9. Characteristics diagram of the wavefronts.

7. Conclusion

Some methods have been presented in this paper to overcome the limitation of the Lundberg equations. One is established in the time domain and the other is in frequency domain. This latter is more difficult to use to recover accurately a strain from some measurements. The time 3-gauges method is in the same spirit as the Lundberg one: it gives a relation between the required signal and the recorded signals. If the time 3-gauges method is less general because it can only recover a strain in one section, it has no limitation and allows recovery of the strain exactly where it is necessary. This reconstruction is associated with a "direct problem", i.e. a well-conditioned problem: that is why these new equations are useful.

This method is compared with the BCGO method, which performs some optimal results as regards the noise measurement. The time 3-gauges method finally gives near similar results as the BCGO ones and is far too simpler to implement. Note that BCGO method allows the reconstruction at any section: but, we recall again that it is not important for an application to the bloc-bar device or to the SHPB set-up.

Acknowledgement

The authors benefited from many useful discussions with Dr. G. Gary at Laboratoire de Mécanique du Solide (Ecole Polytechnique, Palaiseau).

Appendix A

The wave equation in one-dimensional medium is:

$$\frac{\partial^2 u}{\partial x^2} - \frac{1}{c_0^2}\frac{\partial^2 u}{\partial t^2} = 0$$

where $u(x,t)$ is the displacement.

Classically, the solution is:

$$u(x,t) = f(x - c_0 t) + g(x + c_0 t)$$

We can identify

- $f(x - c_0 t)$ as an incident wave $u^{\mathrm{i}}(x,t)$,
- $g(x + c_0 t)$ as a reflected wave $u^{\mathrm{r}}(x,t)$.

Then $u(x,t) = u^{\mathrm{i}}(x,t) + u^{\mathrm{r}}(x,t)$: this relation will greatly help us to demonstrate Eq. (6). Moreover, the strain $\epsilon(x,t)$ verifies the wave equation and can also be decomposed into incident and reflected strain waves:

$$\epsilon_0(t) = \epsilon_0^{\mathrm{i}}(x,t) + \epsilon_0^{\mathrm{r}}(x,t)$$

with:

$$\epsilon_0^{\mathrm{i}}(t) = \epsilon_A^{\mathrm{i}}(t + T_A) = \epsilon_A(t + T_A) - \epsilon_A^{\mathrm{r}}(t + T_A) = \epsilon_A(t + T_A) - \epsilon_C^{\mathrm{r}}(t \underbrace{+ T_A - (T_C - T_A)}_{T_C^{\mathrm{i}}}) \tag{A.1}$$

$$\epsilon_0^{\mathrm{r}}(t) = \epsilon_B^{\mathrm{r}}(t - T_B) = \epsilon_B(t - T_B) - \epsilon_B^{\mathrm{i}}(t - T_B) = \epsilon_B(t - T_B) - \epsilon_C^{\mathrm{i}}(t \underbrace{- T_B + (T_C - T_B)}_{T_C^{\mathrm{r}}}) \tag{A.2}$$

Those relations are illustrated in Fig. 9(a).

If the point C is chosen such as:

$$T_C^{\mathrm{i}} = T_C^{\mathrm{r}}$$

i.e. such as:

$$T_C = \frac{x_C}{c_0} = T_B + T_A = \frac{x_A}{c_0} + \frac{x_B}{c_0} \tag{A.3}$$

we then obtain:

$$\begin{aligned}\epsilon_0(t) &= \epsilon_0^{\mathrm{i}}(t - 2T) + \epsilon_0^{\mathrm{r}}(t - 2T)\\ &= \epsilon_A(t + T_A) + \epsilon_B(t - T_B) - \epsilon_C^{\mathrm{i}}(t + 2 \times T_A - T_C) - \epsilon_C^{\mathrm{r}}(t - 2 \times T_B + T_C)\\ &= \epsilon_A(t + T_A) + \epsilon_B(t - T_B) - \epsilon_C(t + T_A - T_B)\end{aligned} \tag{A.4}$$

Relations between strain and velocity are well-known Johnson (1972):

$$\epsilon^{\mathrm{i}} = \frac{\partial u^{\mathrm{i}}}{\partial x} = \frac{\partial}{\partial x}(f(x - c_0 t)) = -\frac{1}{c_0}\frac{\partial}{\partial t}(f(x - c_0 t)) = -\frac{1}{c_0} v^{\mathrm{i}} \tag{A.5}$$

$$\epsilon^{\mathrm{r}} = \frac{\partial u^{\mathrm{r}}}{\partial x} = \frac{\partial}{\partial x}(g(x + c_0 t)) = \frac{1}{c_0}\frac{\partial}{\partial t}(g(x + c_0 t)) = \frac{1}{c_0} v^{\mathrm{r}} \tag{A.6}$$

then

$$v(x,t) = v^{i}(x,t) + v^{r}(x,t) = c_0(-\epsilon^{i}(x,t) + \epsilon^{r}(x,t)) \tag{A.7}$$

With the help of Eqs. (A.1), (A.2), (A.3) and (A.7), we then deduce the following relation:

$$v_0(t) = c_0(-\epsilon_A(t+T_A) + \epsilon_B(t-T_B)) + v_C(t+T_A-T_B) \tag{A.8}$$

In the same way and with the help of Fig. 9(b), it is easy to prove the two following relations:

$$\epsilon_0(t) = \epsilon_A(t-T_A) + \epsilon_B(t+T_B) - \epsilon_C(t+T_B-T_A) \tag{A.9}$$

$$\frac{v_0(t)}{c_0} = \epsilon_A(t-T_A) - \epsilon_B(t+T_B) + \frac{v_C(t+T_B-T_A)}{c_0} \tag{A.10}$$

Then, from Eqs. (A.4), (A.9), (A.8) and (A.10), the symmetric equations are deduced:

$$\epsilon_0(t) = \frac{1}{2}\left\{\epsilon_A(t-T_A) + \epsilon_A(t+T_A) + \epsilon_B(t-T_B) + \epsilon_B(t+T_B) - \epsilon_C(t+T_B-T_A) - \epsilon_C(t-T_B+T_A)\right\}$$

$$\frac{v_0(t)}{c_0} = \frac{1}{2}\left\{\epsilon_A(t-T_A) - \epsilon_A(t+T_A) + \epsilon_B(t-T_B) - \epsilon_B(t+T_B) + \frac{v_C(t+T_B-T_A)}{c_0} + \frac{v_C(t-T_B+T_A)}{c_0}\right\}$$

References

Bacon, C., 1999. Separation at waves propagating in an elastic or viscoelastic hopkinson pressure bar with three-dimensional effects. International Journal of Impact Engineering 22, 55–69.

Bussac, M.-N., Collet, P., Gary, G., Othman, R., 2002. An optimisation method for separating and rebuilding one-dimensional dispersive waves from multi-point measurements, application to elastic or viscoelastic bar. Journal of Mechanical and Physics of Solids 50, 321–350.

Davies, R., 1948. A critical study of the hopkinson pressure bar. Philosophical Transactions A 240, 375–457.

Dharan, C., Hauser, F., 1970. Determination of stresses–strain characteristics at very high strain rates. Experimental Mechanics 10 (9), 370–376.

Follansbee, P., Frantz, C., 1983. Wave propagation in the split hopkinson pressure bar. Journal of Engineering Materials and Technology 105 (1), 61–66.

Gorham, D., Pope, P., Field, J., 1992. An improved method for compressive stress–strain measurements at very high stain rates. Proceedings of the Royal Society of London Series A 438, 153–170.

Hopkinson, B., 1914. A method for measuring the pressure in the detotion of high explosives or by the impact of bullets. Philosophical Transactions of the Royal Society of London Series A 213, 437–452.

Jacquelin, E., Hamelin, P., 2001. Block-bar device for energy absorption analysis. Mechanical System and Signal Processing 15 (3), 603–617.

Johnson, W., 1972. Impact strength of materials. Edward Arnold.

Kolsky, H., 1963. Stress waves in solids. Clarendon Press.

Lundberg, B., Henchoz, A., 1977. Analysis of elastic waves from two-point strain measurement. Experimental Mechanics 17 (6), 213–218.

Othman, R., Bussac, M.-N., Collet, P., Gary, G., 2001. Séparation et reconstruction des ondes dans les barres élastiques et viscoélastiques à partir de mesures redondantes. Comptes Rendus de l' Academie des Sciences tome 329, Série II b-, 369–376.

Park, S., Zhou, M., 1999. Separation of elastic waves in split hopkinson bars using one point strain measurements. Experimental Mechanics 39, 287–294.

Zhao, H., Gary, G., 1997. A new method for the separation of waves, application to the SHPB technique for an unlimited duration of measurement. Journal of Mechanical Physics and Solids 45 (7), 1185–1202.